Multipole approach to metamaterials

J. Petschulat,[1] C. Menzel,[2] A. Chipouline,[1] C. Rockstuhl,[2] A. Tünnermann,[1,*] F. Lederer,[2] and T. Pertsch[1]

[1]*Institute of Applied Physics, Friedrich Schiller University Jena, Max-Wien-Platz 1, D-07743 Jena, Germany*
[2]*Institute for Solid State Theory and Optics, Friedrich Schiller University Jena, Max-Wien-Platz 1, D-07743 Jena, Germany*

An analytical description for plane-wave propagation in metamaterials is presented. It follows the usual approach for describing light propagation in homogeneous media on the basis of Maxwell's equations, although applied to a medium composed of metallic nanostructures. Here, as an example, these nanostructures are double (or cut) wires. In the present approach it is assumed that the carriers perform collective oscillations in a single wire. These oscillations are coupled to those in the adjacent wire; thus, the internal carrier dynamics may be described by a coupled-oscillator model. The multipole expansion technique is used to account for the electric and magnetic dipole as well as the electric quadrupole moments of these carrier oscillations within the nanostructure. It turns out that the symmetric normal mode is related to the electric dipole moment whereas the antisymmetric normal mode evokes simultaneously a magnetic dipole and an electric quadrupole moment. It is shown how effective permittivity and permeability can be derived from analytical expressions for the dispersion relation, the magnetization, and the electric displacement field. The results of the analytical model are compared with rigorous simulations of Maxwell's equations yielding the limitations and the domain of applicability of the proposed model.

PACS number(s): 42.70.−a, 78.20.Ci, 78.67.Bf, 41.20.Jb

I. INTRODUCTION

Since optical research has been extended toward mesoscopic light-matter interactions, plasmonic effects have become one of the hottest topics in modern optics. New fundamental phenomena in the field of nanoplasmonics have been observed, such as, e.g., extraordinary light transmission in subwavelength apertures [1], interaction of light with nanoscale metallic inclusions [2], and various nonlinear effects due to strong field localization at metal nanoparticles [3]. Probably the most appealing aspect in this research field is the possibility to incorporate metallic nanostructures into a dielectric host medium and to control the dispersive dielectric and magnetic properties of the resulting composite material, at least to a certain extent, at will. The effective properties of these materials can be engineered by varying the size, shape, and material of the nanostructures. To reasonably apply a homogenization procedure [4] to these composite materials, the metallic inclusions and the period of their arrangement have to be much smaller than the incoming wavelength. This requirement is usually not strictly satisfied because the size of typical nanostructures is only about 3–5 times smaller than the wavelength. Nevertheless, it makes sense to apply this homogenization procedure, which compares to the transition from the microscopic to the macroscopic Maxwell's equations, but on the next higher level, in order to simplify the description of light propagation in such composite materials in resorting to plane waves as the relevant normal modes. Comparison with rigorous simulations and experiments must be performed to define the applicability limits of the corresponding effective medium model and to disclose, and subsequently to prevent, additional effects

such as arising from higher-order Bloch modes and nonlocal interactions.

In contrast to naturally available media, the optical response of such peculiar composite materials is determined by both the electrical (permittivity) and the magnetic properties (permeability). These materials, which show significant dispersion in the permittivity and permeability in certain frequency ranges, are usually termed metamaterials (MMs). The combination of basic theoretical works [5–7] with modern manufacturing technologies led to the successful realization of MMs at microwave frequencies at first [8]. During recent years MMs have also been realized in the optical domain [9–12].

The MM design in the optical domain is mainly carried out using rigorous Maxwell's equation solvers like finite-difference time-domain simulations [13], finite-element methods [14], and Fourier modal methods (FMMs) [15]. Instead of these differential methods, integral ones, such as, e.g., the boundary-element method [16], can be used. The discrete-dipole approximation [17] and the multiple multipole method [18] are more physical techniques, where the structure is represented by localized electric multipoles. Nevertheless, presently differential descriptions dominate in MM design.

In contrast to such numerical techniques, the analytical description of MMs is much less developed. Up to now only a few fundamental papers have been published. Podolskiy *et al.* introduced the coupled-dipole equations in order to approximate single and coupled metal wires [19,20]. The direct excitation of *LC* resonances with the magnetic field of the incident plane wave in a system of two coupled rods has been proposed in [21] in order to explain the observed phenomena in terms of effective parameters. Following the effective medium theory, an investigation of dielectric and magnetic conducting inclusions has been performed for spheroids [22]. In spite of the fact that the approach is basically limited to the realm of quasistatics, the model was ex-

tended to describe dynamical problems. In order to simulate the current distribution in a coupled-wire structure and to calculate the permeability, the Green's function technique has also been applied [23]. The application of *RLC* circuit theory has been recently used to obtain the resonance frequencies and the quality factors of coupled split-ring resonators [24].

In this paper an analytical description of the double-wire geometry is presented based on a multipole expansion beyond the standard electric dipole approximation. The model accounts for electric dipole, electric quadrupole, and magnetic dipole contributions appearing upon interaction of charges with the electric field of the incoming plane wave. By this approach, Maxwell's equations can be self-consistently solved and the effective parameters of the MM can be expressed in analytical form. It is shown that the electric quadrupole term has to be retained in this model provided that the magnetic dipole moment is taken into consideration. To describe the internal charge dynamics a coupled-oscillator model has been adapted, which leads to only Lorentzian-shaped solutions. This, in turn, yields expressions which automatically obey the Kramers-Kronig dispersion relations, a compulsory criterion for effective parameters [25].

The paper is organized as follows. Section II is dedicated to the expansion of Maxwell's equations up to the electric quadrupole and magnetic dipole moments. Section III introduces the coupled-oscillator model, while in Sec. IV the normal modes (plane waves) of the respective Maxwell's equations are derived. In Sec. V effective parameters (effective permittivity and permeability) are elaborated using the previously developed formalism. A qualitative comparison between numerically calculated dispersion relations and the derived analytical expression is performed in Sec. VI. A short Summary and Outlook that recapitulates the approximations and considers possible strategies for further work and potential improvements of the method conclude the paper.

II. MACROSCOPIC MAXWELL'S EQUATIONS AND HIGHER-ORDER MULTIPOLES

One of the basic problems in the physics of metamaterials is the homogenization in a medium with small metallic inclusions, i.e., the introduction of an effective medium. If this homogenization is successful, the corresponding normal modes are plane waves obeying a dispersion relation which might be rather involved. This procedure resembles the transition from the microscopic to the macroscopic Maxwell's equations, but now on a second level. Here, we have to average over an ensemble of inclusions (meta-atoms) to arrive at a new homogeneous material, the metamaterial. To avoid confusion it has to be noted that the conventional macroscopic Maxwell' equations hold still in these nanoparticle down to sizes of a few nanometers. An effective medium approach based on the macroscopic (averaged) Maxwell's equations provides a good approximation in the case when the field remains almost unchanged in the volume of averaging. This requirement is well satisfied in condensed matter, where the averaging procedure is performed over volumes

with dimensions much smaller than the wavelength. At the same time the volumes contain a large number of atoms or molecules. For example, for a wavelength of about 1 μm the averaged volume should, rigorously speaking, not exceed 10^{-3} μm^3. Taking into account typical concentrations of about 10^{23} atoms/cm^3, the number of atoms in the volume is about 10^8. For metamaterials, where metallic inclusions play the role of atoms or molecules, the averaging procedure is more involved: typical sizes of the metallic inclusions are just 3–5 times smaller than the wavelength (in the optical domain), and the same averaged volume 10^{-3} μm^3 does not contain a single metallic nanoinclusion. Strictly speaking, this prohibits application of the homogenization procedure for these compounds. Nevertheless, it makes sense to apply the homogenization formalism involving the multipole expansion beyond the dipole approximation and to compare the results with rigorous numerical calculations. This is backed by the fact that in this framework the details of the nanoparticle geometry are mapped onto the dipole, quadrupole, and magnetic dipole moments and an analytical solution can be obtained rather straightforwardly.

A typical strategy for getting a medium with strong dielectric and magnetic dispersion, exhibiting potentially a negative refractive index, is to use metallic nanostructures of a specific shape. These nanostructures have been modelled and manufactured in various geometries [11,12,26]. The reason for using metallic nanostructures is the possibility of exciting localized plasmon polaritons (LPPs), collective excitations of the free-electron gas confined in the metal nanostructure and the field in the surrounding dielectric [27]. Such excitations are characterized by their charge and field distributions. The periodic or randomly distributed metallic structures incorporated in a dielectric host represent the composite medium. An effective permittivity and an effective permeability can be assigned to this medium, which in this case is regarded as a homogeneous effective medium.

Thus MMs are a particular subcategory of effective media that influence both the electric and magnetic fields, with the potential to evoke negative refraction. It is important to emphasize that the magnetic response of the effective medium is caused by the interaction of the electric field with the confined carriers [28]. The incoming electromagnetic wave will inevitably lose energy by the excitation of LPPs. Moreover, as will be seen below, the introduction of permittivity and permeability for MMs is not straightforward since the electric as well as the magnetic response are consequences of the same effect, i.e., the LPP excitation by the electric field. Nevertheless, the effective permittivity and permeability can be unambiguously introduced in the framework of the presented model.

The multipole expansion technique provides a tool to calculate the dispersion relation of the normal mode in the effective medium under consideration. In order to calculate the multipoles, it is suggested to model the LPP charge dynamics by two eigenmodes of coupled harmonic oscillators and then to start the analytical treatment. This "bottom-up" approach means that the macroscopic effective medium parameters are elaborated from the microscopic ones using an idealized but physical model.

The detailed derivation starts with the averaged Maxwell's equations

$$\boldsymbol{\nabla} \times \mathbf{E}(\mathbf{R},t) + \frac{\partial \mathbf{B}(\mathbf{R},t)}{\partial t} = \mathbf{0}, \quad \boldsymbol{\nabla} \cdot \mathbf{D}(\mathbf{R},t) = 0,$$

$$\boldsymbol{\nabla} \times \mathbf{H}(\mathbf{R},t) - \frac{\partial \mathbf{D}(\mathbf{R},t)}{\partial t} = \mathbf{0}, \quad \boldsymbol{\nabla} \cdot \mathbf{B}(\mathbf{R},t) = 0. \quad (1)$$

The medium fields $\mathbf{D}(\mathbf{R},t)$ and $\mathbf{H}(\mathbf{R},t)$ contain electric dipole, electric quadrupole, and magnetic dipole contributions [29]

$$\mathbf{D}(\mathbf{R},t) = \varepsilon_0 \mathbf{E}(\mathbf{R},t) + \mathbf{P}(\mathbf{R},t) - \boldsymbol{\nabla} \cdot \mathbf{Q}(\mathbf{R},t),$$

$$\mathbf{H}(\mathbf{R},t) = \frac{1}{\mu_0}\mathbf{B}(\mathbf{R},t) - \mathbf{M}(\mathbf{R},t). \quad (2)$$

$\mathbf{P}$, $\mathbf{Q}$, and $\mathbf{M}$ represent the electric polarization, the electric quadrupole tensor, and the magnetization, respectively. Capital letters ($\mathbf{R}$) are used for macroscopic coordinates in the averaged Maxwell's equations. The term $[\boldsymbol{\nabla} \cdot \mathbf{Q}(\mathbf{R},t)]_i = \partial Q_{ij}/\partial X_j$ is the divergence of the quadrupole tensor. It is important to take into account both the electric quadrupole and the magnetic dipole terms, because they are of the same order in the multipole expansion series [29,30].

Upon inserting all moments into the material equations, the quasimicroscopic equations can be defined as follows [30]:

$$\mathbf{P}(\mathbf{R},t) = \eta \sum_{k=1}^{N} q_k \mathbf{r}_k(\mathbf{E}(\mathbf{R},t)),$$

$$Q_{ij}(\mathbf{R},t) = \frac{\eta}{2}\sum_{k=1}^{N} q_k [\mathbf{r}_k(\mathbf{E}(\mathbf{R},t))]_i [\mathbf{r}_k(\mathbf{E}(\mathbf{R},t))]_j,$$

$$\mathbf{M}(\mathbf{R},t) = \frac{\eta}{2}\sum_{k=1}^{N} \left[q_k \mathbf{r}_k(\mathbf{E}(\mathbf{R},t)) \frac{\partial}{\partial t} \mathbf{r}_k(\mathbf{E}(\mathbf{R},t)) \right]. \quad (3)$$

The definitions clearly distinguish between microscopic ($\mathbf{r}$) and macroscopic ($\mathbf{R}$) coordinates, q_k represents the charge, N the total number of charges, and η their density. The microscopic coordinates ($\mathbf{r}$) designate the position vectors of the charges in a microscopic coordinate system. The center of the microscopic coordinate system is chosen to be the center of symmetry of the charges.

The reason for the different coordinate systems derives from the averaging procedure for the averaged Maxwell's equations (1). The microscopic coordinates are functions of the electric field and do not appear explicitly in the final expressions. Only one coordinate system, namely, the *macroscopic system of coordinates* $\mathbf{R}$ (i.e., the space coordinate), remains.

III. MULTIPOLE APPROACH FOR THE DOUBLE-WIRE STRUCTURE

Now the multipole expansion is applied to describe the widely used double-wire geometry [9]. As was mentioned above, the microscopic interaction between charges and the
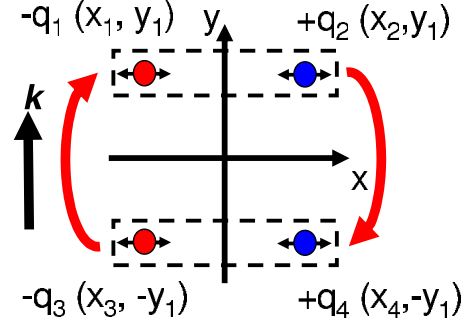
FIG. 1. (Color online) Double-wire MM geometry and corresponding suitable charge distributions that support electric dipole, electric quadrupole, and magnetic dipole moments. The dynamics including interactions between the top and the bottom wires is described by a coupled harmonic oscillator model which is indicated by the red (gray) arrows.

electromagnetic wave is determined by the interaction with the electric field. The interaction with the magnetic field becomes significant only for relativistic velocities or extremely large magnetic fields [31] which are irrelevant in the present study. Under these restrictions the damped and driven harmonic oscillator equation, describing the dynamics of the charge q_k, takes the following form [32]:

$$\frac{\partial^2 \mathbf{r}_k(t)}{\partial t^2} + \gamma_k \frac{\partial \mathbf{r}_k(t)}{\partial t} + \omega_k^2 \mathbf{r}_k(t)$$

$$= \frac{q_k}{m_k}\left[\mathbf{E}(\mathbf{R},t) + \left(\frac{\partial \mathbf{r}_k(t)}{\partial t} \times \mathbf{B}(\mathbf{R},t) \right) \right] \approx \frac{q_k}{m_k}\mathbf{E}(\mathbf{R},t). \quad (4)$$

In Eq. (4) γ_k represents the damping constant and ω_k the eigenfrequency of the charge in the microscopic coordinates $\mathbf{r}_k(t)$. This set of equations of motion can be analytically solved and the system parameters can be evaluated phenomenologically by comparison with experimental or numerical data.

To apply this model to the double-wire geometry we propose the charge arrangement as shown in Fig. 1:

$$\mathbf{r}_1 = \begin{pmatrix} x_1 \\ y_1 \\ 0 \end{pmatrix}, \quad \mathbf{r}_2 = \begin{pmatrix} -x_1 \\ y_1 \\ 0 \end{pmatrix}, \quad \mathbf{r}_3 = \begin{pmatrix} -x_2 \\ -y_1 \\ 0 \end{pmatrix}, \quad \mathbf{r}_4 = \begin{pmatrix} x_2 \\ -y_1 \\ 0 \end{pmatrix},$$

$$q_1 = q_4 = q, \quad q_2 = q_3 = -q. \quad (5)$$

Thus the double-wire geometry is modeled by four charges where the two upper and the two lower ones represent electric dipoles. One important detail of the charge arrangement has to be mentioned explicitly, namely, the introduced asymmetry of the charge dynamics in the top and bottom wires (Fig. 1). The asymmetry has its origin in the finite size of the charge distribution and the spatial retardation of the exciting electric field, i.e., the field is different at both dipole sites, which will be considered in the coupled-oscillator approach. This difference occurs due to the phase and amplitude variation of the electric field propagating along the y direction

between the wires. The interplay of the external field with the induced local field excited in the wires results in the excitation of symmetric and antisymmetric dipole moments in the upper and lower wires. It is worth noting that the required asymmetry to excite second-order multipoles can also be modeled by different oscillator properties (e.g., the damping constant) which will be discussed in detail elsewhere. By substituting Eq. (5) into Eq. (3), the electric dipole, the electric quadrupole, and the magnetic dipole moment can be calculated straightforwardly:

$$\mathbf{P}(\mathbf{R},t) = 2\eta q \begin{pmatrix} x_1 + x_2 \\ 0 \\ 0 \end{pmatrix},$$

$$\mathbf{Q}(\mathbf{R},t) = \eta q y_1 \begin{pmatrix} 0 & x_1 - x_2 & 0 \\ x_1 - x_2 & 0 & 0 \\ 0 & 0 & 0 \end{pmatrix}, \quad (6)$$

$$\mathbf{M}(\mathbf{R},t) = -\eta q y_1 \begin{pmatrix} 0 \\ 0 \\ \dfrac{\partial x_1}{\partial t} - \dfrac{\partial x_2}{\partial t} \end{pmatrix}.$$

From Eqs. (6) one can recognize that all second-order expansion moments (the electric quadrupole and the magnetic dipole moment) vanish for a symmetric charge configuration $x_1 = x_2$, while the polarization (electric dipole) is still nonzero. The symmetric system ($x_1 = x_2$) would consist of two classical dipoles with no influence of higher-order multipoles, and hence with no magnetization.

The coupling of the two oscillators, i.e., the influence of the field generated by the plasmon dynamics, can be considered by introducing an empirical coupling constant σ. For a polarization along the wire axis (x direction) the complete equations describing the charge dynamics in the two wires with the pair center at y simplify to

$$\frac{\partial^2 x_1(t)}{\partial t^2} + \gamma \frac{\partial x_1(t)}{\partial t} + \omega_0^2 x_1(t) - \sigma x_2(t) = \frac{q}{m} E_{1x}(y + y_1, t),$$

$$\frac{\partial^2 x_2(t)}{\partial t^2} + \gamma \frac{\partial x_2(t)}{\partial t} + \omega_0^2 x_2(t) - \sigma x_1(t) = \frac{q}{m} E_{2x}(y - y_1, t). \quad (7)$$

The inhomogeneous solution to the system (7) can be obtained in the Fourier domain $[x(t) \rightarrow \tilde{x}(\omega) e^{-i\omega t}]$ as

$$\tilde{x}_1(\omega) = \frac{q}{m} \frac{\tilde{E}_{1x}(y+y_1,\omega)(i\gamma\omega + \omega^2 - \omega_0^2) - \sigma \tilde{E}_{2x}(y-y_1,\omega)}{\sigma^2 - (i\gamma\omega + \omega^2 - \omega_0^2)^2},$$

$$\tilde{x}_2(\omega) = \frac{q}{m} \frac{\tilde{E}_{2x}(y+y_1,\omega)(i\gamma\omega + \omega^2 - \omega_0^2) - \sigma \tilde{E}_{1x}(y-y_1,\omega)}{\sigma^2 - (i\gamma\omega + \omega^2 - \omega_0^2)^2}. \quad (8)$$

Evidently, because of Eq. (6), only the expressions $x_1 + x_2$ and $x_1 - x_2$ enter the formalism,

$$\tilde{x}_1(\omega) + \tilde{x}_2(\omega) = \frac{q}{m} \frac{\tilde{E}_{1x}(y+y_1,\omega) + \tilde{E}_{2x}(y-y_1,\omega)}{\omega_0^2 - \omega^2 - i\gamma\omega - \sigma}$$

$$\equiv [\tilde{E}_{1x}(y+y_1,\omega) + \tilde{E}_{2x}(y-y_1,\omega)]\chi^+(\omega),$$

$$\tilde{x}_1(\omega) - \tilde{x}_2(\omega) = \frac{q}{m} \frac{\tilde{E}_{1x}(y+y_1,\omega) - \tilde{E}_{2x}(y-y_1,\omega)}{\omega_0^2 - \omega^2 - i\gamma\omega + \sigma}$$

$$\equiv [\tilde{E}_{1x}(y+y_1,\omega) - \tilde{E}_{2x}(y-y_1,\omega)]\chi^-(\omega), \quad (9)$$

where we have introduced the substitution

$$\chi^\pm(\omega) = \frac{q}{m} \frac{1}{(\omega_0^2 - \omega^2 - i\gamma\omega \pm \sigma)}. \quad (10)$$

The dependence of the oscillation amplitudes on the electric field in the upper $[\tilde{E}_{1x}(y+y_1,\omega)]$ and bottom wires $[\tilde{E}_{2x}(y-y_1,\omega)]$ can be transformed into a dependence on the field at the center between both wires by taking the retardation into account:

$$\tilde{E}_{1x}(y+y_1,\omega) = \tilde{E}_{0x}(\omega)e^{ik(y+y_1)} = \tilde{E}_x(y,\omega)e^{iky_1},$$

$$\tilde{E}_{1x}(y-y_1,\omega) = \tilde{E}_{0x}(\omega)e^{ik(y-y_1)} = \tilde{E}_x(y,\omega)e^{-iky_1}. \quad (11)$$

At this point we explicitly mention that in our model the excitation via plane waves is described in an approximate manner. The electric field propagating from the first to the second wire is determined by k, the complex wave number. In addition to this external electric field evolution, the excitation process is also governed by the near-field coupling of the two wires. This mechanism is taken into account by the empirical coupling constant σ between the two wires and not by the additional electric fields on the right side of Eq. (11). This approximation provides an analytical solution for the equations of motion and prevents us from regarding the complex near-field interactions between the wires by introducing that coupling constant. Therefore k represents the propagation vector of the corresponding effective medium, not the free-space wave vector. Upon substitution into Eq. (9), the oscillation amplitudes depend only on the electric field at a single site required for performing the multipole expansion,

$$\tilde{x}_1(\omega) + \tilde{x}_2(\omega) = 2\tilde{E}_x(y,\omega)\cos(k_y y_1)\chi^+(\omega),$$

$$\tilde{x}_1(\omega) - \tilde{x}_2(\omega) = 2i\tilde{E}_x(y,\omega)\sin(k_y y_1)\chi^-(\omega). \quad (12)$$

The quantities $\chi^\pm(\omega)$ introduced above represent the polarizabilities related to the eigenmodes of the coupled system, where the $(+)$ and the $(-)$ signs indicate the symmetric and the antisymmetric modes, respectively. It turns out that the antisymmetric mode induces both the magnetic dipole and the electric quadrupole moments, whereas the symmetric mode is related to the electric dipole moment. Now the calculated multipole moments (6) can be rewritten

$$\widetilde{\mathbf{P}}(y,\omega) = 2q\,\eta \begin{pmatrix} 2\chi^+(\omega)\cos(k_y y_1) \\ 0 \\ 0 \end{pmatrix} \widetilde{E}_x(y,\omega),$$

$$\widetilde{\mathbf{Q}}(y,\omega)$$
$$= \eta q y_1 \begin{pmatrix} 0 & 2i\chi^-(\omega)\sin(k_y y_1) & 0 \\ 2i\chi^-(\omega)\sin(k_y y_1) & 0 & 0 \\ 0 & 0 & 0 \end{pmatrix} \widetilde{E}_x(y,\omega),$$

$$\widetilde{\mathbf{M}}(y,\omega) = i\omega q y_1 \eta \begin{pmatrix} 0 \\ 0 \\ 2i\chi^-(\omega)\sin(k_y y_1) \end{pmatrix} \widetilde{E}_x(y,\omega). \quad (13)$$

IV. THE DISPERSION RELATION OF PLANE WAVES IN A DOUBLE-WIRE SYSTEM

For a plane wave propagating along the positive y axis and with an electric field polarized along the x direction, the set of Maxwell's equations can be simplified. The Maxwell curl equations reduce to

$$\frac{\partial \widetilde{E}_x(y,\omega)}{\partial y} = -i\omega \widetilde{B}_z(y,\omega), \quad (14)$$

and, taking into account Eq. (2),

$$\frac{\partial \widetilde{B}_z(y,\omega)}{\partial y} = \mu_0 \frac{\partial \widetilde{D}_x(y,\omega)}{\partial t} + \mu_0 \frac{\partial \widetilde{M}_z(y,\omega)}{\partial y}$$
$$= -i\omega\mu_0 \left(\varepsilon_0 \widetilde{E}_x(y,\omega) + \widetilde{P}_x(y,\omega) - \frac{\partial \widetilde{Q}_{xy}(y,\omega)}{\partial y} \right)$$
$$+ \mu_0 \frac{\partial \widetilde{M}_z(y,\omega)}{\partial y}. \quad (15)$$

Differentiating Eq. (14) with respect to y and substituting (15) into the right side of the (14) results in

$$-\frac{\partial^2 \widetilde{E}_x(y,\omega)}{\partial y^2} = \omega^2\mu_0 \left(\varepsilon_0 \widetilde{E}_x(y,\omega) + \widetilde{P}_x(y,\omega) - \frac{\partial \widetilde{Q}_{xy}(y,\omega)}{\partial y} \right)$$
$$+ i\omega\mu_0 \frac{\partial \widetilde{M}_z(y,\omega)}{\partial y}. \quad (16)$$

Finally, the substitution of the electric and magnetic multipoles (13) provides a self-consistent equation for the x component of the electric field,

$$-\frac{\partial^2 \widetilde{E}_x(y,\omega)}{\partial y^2} = \omega^2\mu_0 \left(\varepsilon_0 \widetilde{E}_x(\omega) + 4\eta q \chi^+(\omega)\cos(k_y y_1)\widetilde{E}_x(y,\omega) - 2i\,\eta q y_1 \chi^-(\omega)\sin(k_y y_1)\frac{\partial \widetilde{E}_x(y,\omega)}{\partial y} \right)$$
$$- 2i\omega^2\mu_0 \eta q y_1 \chi^-(\omega)\sin(k_y y_1)\frac{\partial \widetilde{E}_x(y,\omega)}{\partial y}. \quad (17)$$

It is interesting to note that the magnetic dipole and electric quadrupole contributions are identical. This is another proof that the electric quadrupole and magnetic dipole contributions have the same order of magnitude and both (not only the magnetic dipole term) have to be taken into account simultaneously. The dispersion relation for the plane wave can be found straightforwardly by plugging the ansatz $\widetilde{E}_x(y,\omega) = \widetilde{E}_{0x}(\omega)e^{ik_y y}$ into Eq. (17),

$$k_y^2(\omega) = \frac{\omega^2}{c^2}[1 + A\chi^+(\omega)\cos(k_y y_1) + A\chi^-(\omega)y_1 k_y \sin(k_y y_1)],$$

$$A \equiv \frac{4\eta q}{\varepsilon_0}. \quad (18)$$

The implicit dispersion relation obtained can be solved only numerically. To keep the model analytical, we can approximate the trigonometric functions $\cos(k_y y_1)$ and $\sin(k_y y_1)$ for small arguments $k_y y_1 \ll 1$:

$$\cos(k_y y_1) \approx 1 - \frac{(k_y y_1)^2}{2}, \quad \sin(k_y y_1) \approx k_y y_1,$$

$$k_y^2 = \frac{\omega^2}{c^2}\frac{1 + A\chi^+(\omega)}{1 + \frac{\omega^2}{c^2}Ay_1^2\left(\frac{1}{2}\chi^+(\omega) - \chi^-(\omega)\right)}. \quad (19)$$

Now with Eq. (19) the dispersion relation is explicit in k_y and mirror symmetric with respect to $k_y=0$, as in Eq. (18). The above approximation is justified because $y_1 \ll \lambda$ holds in the considered cut-wire geometry.

V. EFFECTIVE PARAMETERS

In this section the model is used to derive effective parameters. The strategy is to show that both quantities (permittivity and permeability) can be derived independently while the resulting propagation constant

$$k_{\text{eff}}^2 = \frac{\omega^2}{c^2}\varepsilon_{\text{eff}}\mu_{\text{eff}} \equiv k_y^2 \tag{20}$$

must coincide with the dispersion relation Eq. (19). First, the effective permittivity can be introduced using Eq. (2) and substituting Eq. (13),

$$\widetilde{D}_x(y,\omega) = \varepsilon_0\widetilde{E}_x(y,\omega) + \widetilde{P}_x(y,\omega) - \frac{\partial}{\partial y}\widetilde{Q}_{xy}(y,\omega)$$

$$= \varepsilon_0\left(1 + A\chi^+(\omega) - \frac{Ak_y^2y_1^2}{2}[\chi^+(\omega) - \chi^-(\omega)]\right)\widetilde{E}_x(y,\omega)$$

$$\equiv \varepsilon_0\varepsilon_{\text{eff}}(k_y,\omega)\widetilde{E}_x(y,\omega). \tag{21}$$

Thus we obtain

$$\varepsilon_{\text{eff}}(k_y,\omega) = 1 + A\chi^+(\omega) - \frac{Ak_y^2y_1^2}{2}[\chi^+(\omega) - \chi^-(\omega)]. \tag{22}$$

Note that the effective permittivity is spatially dispersive, i.e., ε_{eff} is a function of the propagation vector itself. This is caused by the nonvanishing electric quadrupole moment, which enters the equation through the first derivative.

Now we proceed to introduce the effective permeability. For the pertinent field components we write Eq. (2) as

$$\widetilde{H}_z(y,\omega) = \frac{1}{\mu_0}\widetilde{B}_z(y,\omega) - \widetilde{M}_z(y,\omega) \equiv \frac{1}{\mu_{\text{eff}}(\omega)\mu_0}\widetilde{B}_z(y,\omega). \tag{23}$$

In Eq. (23) it is required that the relation $\widetilde{\mathbf{M}}[\widetilde{\mathbf{B}}(\mathbf{R},\omega)]$ is explicitly known. To evaluate this dependence we rewrite the magnetic dipole moment (13) and Maxwell's equations (1) for plane waves,

$$\widetilde{M}_z(y,\omega) = -\frac{\omega}{c^2}\frac{A}{2}y_1^2\chi^-(\omega)k_y\widetilde{E}_x(y,\omega),$$

$$\widetilde{E}_x(y,\omega) = -\frac{\omega}{k_y}\widetilde{B}_z(y,\omega),$$

$$\widetilde{M}_z(y,\omega) = \frac{\omega^2}{c^2}\frac{A}{2}y_1^2\chi^-(\omega)\widetilde{B}_z(y,\omega). \tag{24}$$

Substitution of (24) into (23) results in the desired effective permeability,

$$\mu_{\text{eff}}(\omega) = \frac{1}{1 - \frac{\omega^2}{c^2}\frac{A}{2}y_1^2\chi^-(\omega)}. \tag{25}$$

It is straightforward to show that the product of the two effective quantities, the effective permittivity and effective permeability, satisfies condition (20). Actually, it is not necessary to calculate the permeability separately since the dispersion relation (19) is explicitly known. That is again a fragment of the multipole expansion that leads to a coupling between these two material properties that would be completely decoupled in a purely dipole interaction regime.

This coupling can be interpreted as follows. In our model the interaction of the incoming plane wave with matter is determined only by the electric field (interaction with the magnetic field is negligible). This interaction with the electric field can be expressed in terms of electric and magnetic multipole responses that consequently determine the dependence of all quantities on the electric field. The excitation of coupled-charge oscillations leads to a magnetic response that can be described by an effective magnetic permeability, which is again a consequence of the interaction with the electric (not the magnetic) field. It should be emphasized again that the physical picture of the magnetic response differs basically from that taking place in solid state physics. The magnetic response in the latter case is caused by a magnetic field which induces or aligns existing magnetic moments of atoms or molecules (the free-electron magnetism effect again is caused by interaction with the magnetic components of the field). In the case of MMs the electric field excites LPPs which contribute to both electric and magnetic responses, while the microscopic magnetic component does not participate in the light-matter interaction.

To summarize this section, two issues have to be emphasized.

(1) In the framework of the present model, the effective permittivity and permeability can be unambiguously introduced. Furthermore, the product of the two material parameters reproduces the independently calculated dispersion relation for normally incident plane waves; and both effective parameters are reduced to trivial expressions if the electric quadrupole and the magnetic dipole contributions are set to zero.

(2) The introduction of effective parameters might look artificial because the electric as well as the magnetic response are caused by an interaction of carriers confined in the nanostructure with the electric field [28,36], and are mutually related to each other. However, the decoupling of these two responses, e.g., by introducing permittivity and permeability, might be necessary, for example, for comparing them with numerically determined electric and magnetic properties in terms of ε and μ.

VI. VALIDATION OF THE MODEL

In this section, a quantitative comparison of results obtained by the outlined analytical approach and rigorous numerical calculations is performed. First it is necessary to summarize that the wave vector [Eq. (19)] depends on frequency ω, on the product of the carrier density η with the charge q, on the geometrical parameter y_1, on the two quantities $\chi^+(\omega)$ and $\chi^-(\omega)$ (which are in turn functions of the eigenfrequency ω_0), on the damping constant γ, and on the coupling constant σ of the carrier oscillations.

In order to determine rigorously the dispersion relation of the geometry shown in Fig. 2(a) we have used the Fourier modal method [33]. To describe the propagation of electromagnetic waves in 3D bulk media [see Fig. 2(b)] the calculation has been examined with periodic boundary conditions in all three space dimensions. The periods used in the x, y, and z directions are $\Lambda_x = 600$ nm, $\Lambda_y = 500$ nm, and Λ_z
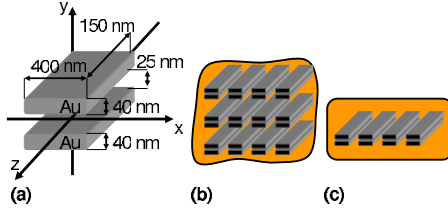
FIG. 2. (Color online) (a) Geometry of the simulated double-wire meta-atom is shown. (b) Three-dimensional (3D) bulk MM alignment to calculate the dispersion relation of a bulk MM and (c) the slab arrangement which allows additionally the calculation of effective parameters.

=150 nm, respectively. The double wires are formed from gold with the sizes shown in Fig. 2(a), and are separated by a thin glass layer with $n=1.44$. The corresponding effective material parameters of the same geometry have been obtained by FMM calculations for one layer [see Fig. 2(c)]. The effective permeability and permittivity are calculated from the complex reflected and transmitted amplitudes which are used in inverted expressions for the reflection and transmission of light at a homogeneous slab [34].

First the dispersion relation of the 3D infinite metamaterial was calculated numerically and the analytical version was fitted to it (Fig. 3). The comparison shows very good agreement in the small-frequency domain, while for larger frequencies the analytical dispersion relation differs from the numerical one. This can be explained by the violation of the subwavelength criterion for larger frequencies. Since no numerical data for the corresponding effective parameters are available due to the absence of boundaries, a finite geometry has been simulated. Therefore Fig. 4(a) shows the effective refractive index that corresponds to the dispersion relation of the slab arrangement as well as the retrieved effective parameters [see Figs. 4(d) and 4(g)]. The second column contains the fitted effective refractive index [Fig. 4(b)] and the following effective parameters [see Figs. 4(e) and 4(h)]. Since only the dispersion relation in terms of the refractive index has been fitted, the coincidence of the effective parameters is significant. Another remarkable property of the analytically determined effective parameters is the vanishing of the anti-resonances. In Fig. 4(g) this feature appears in the effective permeability exactly at the resonance position of the effective permittivity. The same antiresonance appears in the effective permittivity at the resonance position of the effective
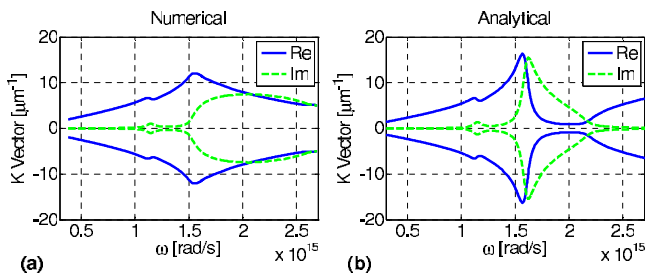
permeability but it is much weaker and cannot be observed in Fig. 4(d). The last column in Fig. 4 shows the effective parameters that are a direct result of the fit of the dispersion relation of the bulk metamaterial, presented in Fig. 3. It can be seen that the resonance positions as well as their absolute values differ from the slab parameters [35]. This can be explained by the coupling of neighboring metamaterial layers, which leads to slightly different effective material parameters from those for a decoupled metamaterial, e.g., a metamaterial slab. In the following we describe the fitting procedure in detail.

First, the locations of both resonances and their bandwidths were fitted. The resonance positions in the analytical model have been tuned by selecting the eigenfrequency ω_0 in between the two resonance frequencies of the numerical dispersion relation. We notice that the eigenfrequency ω_0 corresponds to the localized plasmon-polariton frequency of an isolated wire. The eigenfrequency of such a wire can be estimated with an ellipsoidal particle in the quasistatic regime [27] with the same dimensions shown in Fig. 2(a). The calculated value coincides approximately with the eigenfrequency used for the fit (see the value in parentheses in Table I). To realize the presence of two resonances, the coupling constant σ was increased until the two resonance positions coincide with the numerical ones.

The resonance width, which represents the damping, has been retrieved from the full width at half maximum value of the imaginary part of the peak in the dispersion relation for the 3D geometry and the refractive index for the 2D arrangement. The unknown term Aq/m [this term appears in the expressions for $k(\omega)$, $\varepsilon(\omega)$, and $\mu(\omega)$] represents the only remaining free fitting parameter. The values found for both scenarios are listed in Table I.

While the dispersion relation can be fitted, the permittivity and the permeability are not direct outcomes of the fitting procedure. Having the dispersion relation (and respective constants) fitted, the assigned effective parameters can be calculated from Eqs. (22) and (25) without any further adaptation. The comparison of these functions (refractive index, permittivity, and permeability) validates the procedure introduced for the modeling of effective parameters as well as the application of the multipole expansion (see Fig. 4).

Nevertheless, one can conclude that for such a rather primitive model the analytical results are in quite good agreement with the rigorous simulations, especially for small frequencies (long wavelengths) where the approach based on the averaged Maxwell's equations is supposedly more appropriate.

VII. SUMMARY AND OUTLOOK

The aim of this paper was to develop simple tools for the analytic description of plane-wave propagation in MMs employing mathematical techniques well known in electrodynamics. The calculations are based on the averaged Maxwell's and material equations which retain higher-order multipole terms. In order to model the MM structure, a collective carrier arrangement has been proposed that supports electric dipole, magnetic dipole, and electric quadrupole mo-

FIG. 3. (Color online) (a) Dispersion relation obtained from the numerical calculations in an infinite 3D MM as shown in Fig. 2(b) and the corresponding fitted analytical version (b).
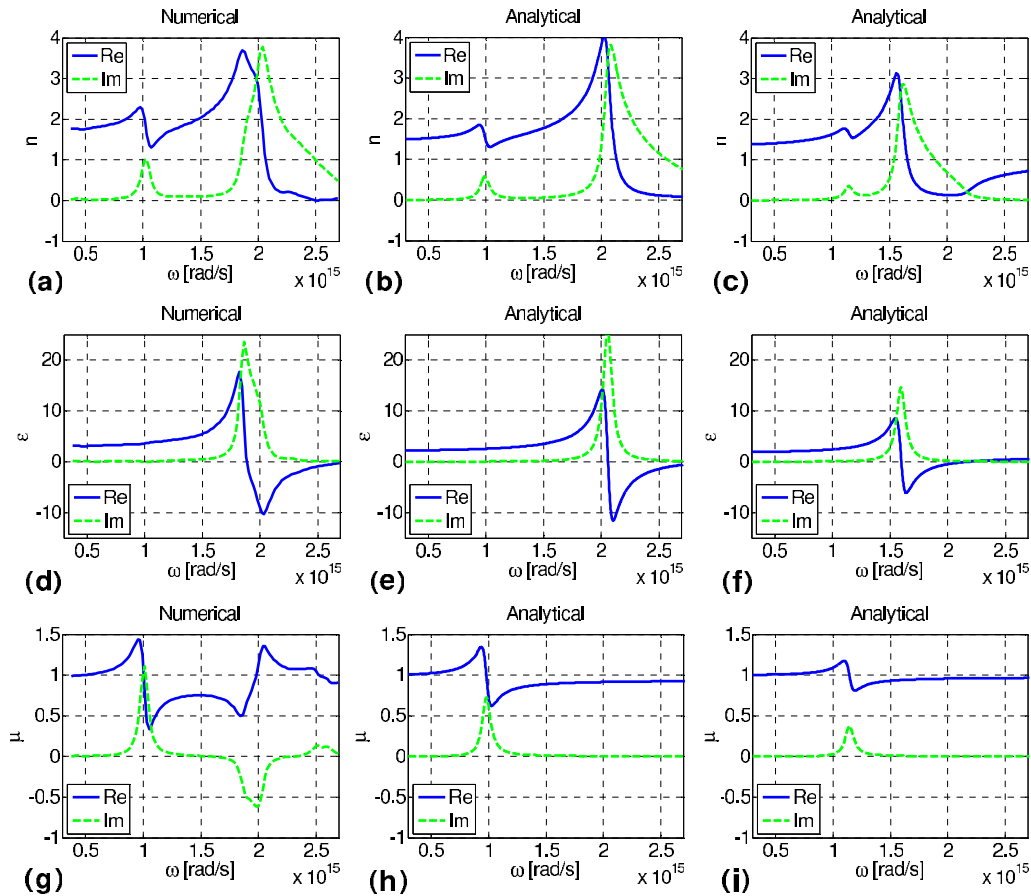
FIG. 4. (Color online) Retrieved effective index (a), effective permittivity (d), and effective permeability (g) from FMM simulations of a 2D single-layer metamaterial. Based on the coefficients from fitting the dispersion relation that is equivalent to the refractive index in the 2D case, the resulting effective index (b), the effective permittivity (e), and the effective permeability (h) resulting from the analytical model are shown. (c), (f), and (i) correspond to the analytically determined effective parameters for the 3D infinite bulk metamaterial. Therefore the dispersion relation (Fig. 3) has been fitted by the analytical one.

ments and mimics qualitatively the LPP dynamics. The charge dynamics and the eigenmodes of the carrier oscillations have been described by using a coupled harmonic oscillator model. It turned out that the symmetric eigenmodes evoke an electrical dipole moment whereas the antisymmetric mode induces both an electrical quadrupole and a magnetic dipole moment. A self-consistent solution for plane waves has been achieved and its dispersion relation has been calculated. The effective permittivity and the permeability have been elaborated based on the material equations and the obtained dispersion relation. It has been shown that the ef-

fective electric and magnetic properties appear to be mutually coupled. Finally, a comparison between numerically calculated and analytically obtained dispersion relations and effective permittivity and permeability parameters has been performed in order to evaluate the applicability of the theory. It has been verified that the main features of the dispersion relation can be reproduced by our analytical model. The effective parameters calculated in the framework of the analytical model display a good qualitative agreement with the ones obtained by the numerical calculations.

TABLE I. The fitting parameters that have been applied to match the dispersion relation for the slab as well as for the bulk arrangement. Together with Eqs. (22) and (25) the effective parameters can be calculated as shown in Fig. 4. Additionally, the eigenfrequencies of the single wire calculated separately in the quasistatic regime are listed in parentheses.

Fitting parameter	Slab MM	Bulk MM
ω_0 (rad/s)	1.62×10^{15} (1.85×10^{15})	1.39×10^{15} (1.85×10^{15})
γ (rad/s)	9.42×10^{13}	9.42×10^{13}
σ (rad/s)	1.60×10^{30}	0.60×10^{30}
Aq/m (A s V/m^2 K g)	5.00×10^{30}	2.20×10^{30}

It is believed that the introduced formalism provides a deeper insight into the description of MMs using quasimicroscopic Maxwell's equations. Due to the approximate nature of the model it is not considered for use for design purposes. The same basic ideas of the model can be applied to other geometries for MMs as well. A detailed work on the analytical description of light propagation in a medium comprising split-ring resonators is presently in progress. A nonlinear material response can be naturally obtained from the quadrupole and magnetic dipole description as well.

[1] T. W. Ebbesen, H. J. Lezec, H. F. Ghaemi, T. Thio, and P. A. Wolff, Nature (London) **391**, 667 (1998).

[2] P. Mühlschlegel, H.-J. Eisler, O. J. F. Martin, B. Hecht, and D. W. Pohl, Science **308**, 1607 (2005).

[3] M. Danckwerts and L. Novotny, Phys. Rev. Lett. **98**, 026104 (2007).

[4] T. C. Choy, *Effective Medium Theory: Principles and Applications* (Oxford University Press, New York, 1999).

[5] V. G. Veselago, Sov. Phys. Usp. **10**, 509 (1968).

[6] J. B. Pendry, A. J. Holden, D. J. Robbins, and W. J. Stewart, IEEE Trans. Microwave Theory Tech. **47**, 2075 (1999).

[7] J. B. Pendry, Phys. Rev. Lett. **85**, 3966 (2000).

[8] D. R. Smith, Willie J. Padilla, D. C. Vier, S. C. Nemat-Nasser, and S. Schultz, Phys. Rev. Lett. **84**, 4184 (2000).

[9] V. M. Shalaev, W. Cai, U. K. Chettiar, H. Yuan, A. K. Sarychev, V. P. Drachev, and A. V. Kildishev, Opt. Lett. **30**, 3356 (2005).

[10] G. Dolling, C. Enkrich, M. Wegener, J. F. Zhou, C. M. Soukoulis, and S. Linden, Opt. Lett. **30**, 3198 (2005).

[11] G. Dolling, M. Wegener, C. M. Soukoulis, and S. Linden, Opt. Lett. **32**, 53 (2007).

[12] U. K. Chettiar, A. V. Kildishev, H.-K. Yuan, W. Cai, S. Xiao, V. P. Drachev, and V. M. Shalaev, Opt. Lett. **32**, 1671 (2007).

[13] K. S. Yee, IEEE Trans. Antennas Propag. **14**, 302 (1966).

[14] A. Taflove and S. C. Hagness, *Computational Electrodynamics*, 3rd ed. (Artech House, Boston, 2005).

[15] L. Li, J. Opt. Soc. Am. A **14**, 2758 (1997).

[16] C. Rockstuhl, M. G. Salt, and H. P. Herzig, J. Opt. Soc. Am. A **20**, 1969 (2003).

[17] B. T. Draine and P. J. Flatau, J. Opt. Soc. Am. A **11**, 1491 (1994).

[18] C. Hafner, *The Generalized Multipole Technique for Computational Electromagnetics* (Artech House, Boston, 1990).

[19] V. A. Podolskiy, A. K. Sarychev, E. Narimanov, and V. M. Shalaev, J. Opt. A, Pure Appl. Opt. **7**, 32 (2005).

[20] A. V. Podolskiy, A. K. Sarychev, and V. M. Shalaev, Opt. Express **11**, 735 (2003).

[21] A. K. Sarychev, G. Shvets, and V. M. Shalaev, Phys. Rev. E **73**, 036609 (2006).

[22] A. N. Lagarkov and A. K. Sarychev, Phys. Rev. B **53**, 6318 (1996).

[23] L. V. Panina, A. N. Grigorenko, and D. P. Makhnovskiy, Phys. Rev. B **66**, 155411 (2002).

[24] T. P. Meyrath, T. Zentgraf, and H. Giessen, Phys. Rev. B **75**, 205102 (2007).

[25] M. I. Stockman, Phys. Rev. Lett. **98**, 177404 (2007).

[26] S. Zhang, W. Fan, N. C. Panoiu, K. J. Malloy, R. M. Osgood, and S. R. J. Brueck, Phys. Rev. Lett. **95**, 137404 (2005).

[27] U. Kreibig and M. Vollmer, *Optical Properties of Metal Clusters* (Springer, Berlin, 1993).

[28] S. Tretyakov, *Analytical Modeling in Applied Electromagnetics* (Artech House, Boston 2003), p. 131.

[29] J. D. Jackson, *Classical Electrodynamics* (Wiley, New York, 1975).

[30] R. E. Raab and O. L. De Lange, *Multipole Theory in Electromagnetism* (Clarendon, Oxford, 2005).

[31] M. Wegener, *Extreme Nonlinear Optics* (Springer, Berlin, 2005).

[32] C. Kittel, *Introduction to Solid State Physics* (Wiley, New York, 1986).

[33] C. Rockstuhl, C. Menzel, T. Paul, T. Pertsch, and F. Lederer (unpublished).

[34] D. R. Smith, D. C. Vier, T. Koschny, and C. M. Soukoulis, Phys. Rev. E **71**, 036617 (2005).

[35] C. Rockstuhl, Thomas Paul, Falk Lederer, Thomas Pertsch, Thomas Zentgraf, Todd P. Meyrath, and Harald Giessen, Phys. Rev. B **77**, 035126 (2008).

[36] C. Rockstuhl, T. Zentgraf, E. Pshenay-Severin, J. Petschulat, A. Chipouline, J. Kuhl, T. Pertsch, H. Giessen, and F. Lederer, Opt. Express **15**, 8871 (2007).